A Compact Cluster of Massive Red Galaxies at a Redshift of 1.51

Patrick J. McCarthy[1], Haojing Yan[1], Roberto G. Abraham[2], Erin Mentuch[2], Karl Glazebrook[3], Lin Yan[4], Hsiao-Wen Chen[5], S. Eric Persson[1], Preethi Nair[2], Sandra Savaglio[6], David Crampton[7], Stephanie Juneau[8], Damien Le Borgne[9], R. G. Carlberg[2] Ronald O. Marzke[10], Inger Jørgensen[11], Kathy Roth[11] Richard Murowinski[7],

ABSTRACT

We describe a compact cluster of massive red galaxies at $z = 1.51$ discovered in one of the Gemini Deep Deep Survey (GDDS) fields. Deep imaging with Near Infrared Camera and Multi Object Spectrometer (NICMOS) on the *Hubble* Space Telescope reveals a high density of galaxies with red optical to near-IR colors surrounding a galaxy with a spectroscopic redshift of 1.51. Mid-IR imaging with Infrared Array Camera (IRAC) on the *Spitzer* Space telescope shows that these galaxies have spectral energy distributions that peak between 3.6μm and 4.5μm. Fits to 12-band photometry reveal 12 or more galaxies with spectral shapes consistent with $z = 1.51$. Most are within $\sim$ 170 co-moving kpc of the GDDS galaxy. Deep F814W images with the Advanced Camera for Surveys (ACS) on HST reveal that these galaxies are a mix of early-type galaxies, disk galaxies and close pairs. The total stellar mass enclosed within a sphere of 170 kpc in radius is $> 8 \times 10^{11} M_\odot$. The colors of the most massive

[1] Observatories of the Carnegie Institution of Washington, 813 Santa Barbara Street, Pasadena, CA 91101

[2] Department of Astronomy & Astrophysics University of Toronto, 50 St. George St. Toronto, ON, M5S 3H4

[3] Centre for Astrophysics & Supercomputing Swinburne University of Technology Mail #31, PO Box 218, Hawthorne, VIC 3122, Australia

[4] Spitzer Science Center, California Institute of Technology, MS 100-22, Pasadena, CA 91125

[5] Dept. of Astronomy & Astrophysics, University of Chicago 5640 South Ellis Ave. Chicago, IL 60637

[6] Max-Planck-Institut für extraterrestrische Physik, Garching, Germany

[7] Herzberg Institute of Astrophysics, National Research Council, 5071 West Saanich Road, Victoria, British Columbia, V9E 2E7, Canada

[8] Steward Observatory University of Arizona Tucson, AZ 85721

[9] DSM/DAPNIA/Service d'Astrophysique CEA/SACLAY 91191 Gif-sur-Yvetta Cedex, France

[10] Dept. of Physics and Astronomy, San Francisco State University, 1600 Holloway Avenue, San Francisco, CA 94132

[11] Gemini Observatory, Hilo, HI 96720

galaxies are close to those expected from passive evolution of simple stellar populations (SSP) formed at much higher redshifts. We suggest that several of these galaxies will merge to form a single, very massive galaxy by the present day. This system may represent an example of a short-lived dense group or cluster core typical of the progenitors of massive clusters in the present day and suggests the red sequence was in place in over-dense regions at early times.

Subject headings: galaxies: evolution, clusters

1. INTRODUCTION

Galaxy clusters provide important laboratories for studies of galaxy evolution. Key aspects of our knowledge concerning the evolution of massive early-type galaxies are derived from the study of rich galaxy clusters at intermediate redshifts (e.g. Stanford et al. (1998); van Dokkum et al. (1998); Kelson et al. (2000)). Cluster studies also provide an important tool for gauging the growth of structure and probing the density of the underlying dark matter and energy (e.g. Springel et al. (2005)). Clusters at $z \sim 1-2$ provide strong leverage in addressing both issues and thus there is considerable interest in find clusters and groups of galaxies at $z \gtrsim 1$.

A variety of survey techniques have proven effective at identifying galaxy clusters to $z \sim 1$ and beyond. X-ray selected samples at $z > 1$, while relatively small, sample the most massive and dynamically relaxed systems (e.g. Rosatti et al. 1998; Stanford et al. 1998). Large area multi-color surveys, such as the red sequence surveys (e.g. Gladders & Yee (2005)) have produced large samples of systems in a range of evolutionary stages. The mid-IR imaging camera on the Spitzer Space Telescope (hereafter Spitzer) has extended the range and power of multi-color surveys and a number of programs are producing confirmed and candidate clusters at $z > 1$ (Stanford et al. 2005, 2006). In this short report we present the discovery of one of the most distant clusters to date. Deep HST and Spitzer images of a massive, passively evolving galaxy identified in the Gemini Deep Deep Survey (GDDS; Abraham et al. (2004)) has led to the detection of a very compact cluster or group of massive red galaxies at of $z = 1.51$. Ultra-deep spectroscopy with Gemini and deep multi-band photometry has allowed us to obtain a firm redshift for a group of galaxies beyond the reach of most spectroscopic studies.

In §2 we present the observations of the galaxy GDDS-12-5869 and its surroundings. In section §3 we will discuss the properties of the surrounding galaxies and in section §4 we will briefly discuss the implications for the formation of massive galaxies. We adopt the following cosmological parameters: $h_o = 0.71$, $\Omega_m = 0.27$ and $\Omega_\Lambda = 0.73$. At $z = 1.5$, $1''$ corresponds to 8.54 kpc.

2. OBSERVATIONS

2.1. Ground-based Imaging and Spectroscopy

Much of the basic observational data used in this current work has been presented in previous papers related to the GDDS. In paper I (Abraham et al. 2004), the visible spectroscopy and supporting optical and near-IR imaging data are described. The optical imaging and early, ground-based near-IR photometry are discussed in more detail in papers describing the parent sample drawn from the Las Campanas Infrared survey (Chen et al. 2002; Firth et al. 2002; McCarthy et al. 2001). In GDDS Paper IV (McCarthy et al. 2004), we analyzed spectra of passively evolving galaxies with $1.3 < z < 2$. One of these objects is GDDS-12-5869, a galaxy at $z = 1.51$ with K(Vega)$= 18.6$ and a moderately red color of $I - K = 2.6$ mag. Our spectrum of this object is shown in Fig. 1 of Paper IV. In the classification scheme of paper I, this object has a high confidence redshift and a spectrum consistent with no recent or ongoing star formation.

2.2. HST ACS Imaging

Approximately 60% of the 120 arcmin^2 GDDS survey area was imaged with the Wide Field Camera of ACS on the HST. The details of the observations are given in paper VIII (Abraham et al. 2007). The 12-hour GDDS field was observed for 14,640 seconds in the F814W band (hereafter I_{814}). The observations were dithered in non-integer pixel steps and a mosaic was constructed using the standard "MultiDrizzle" package (Koekemoer et al. 2002). The mosaic is $\sim 210'' \times 210''$ in extent, and GDDS-12-5869 lies $35''$ from the southern edge of the field.

2.3. HST NICMOS Imaging

Ten passively evolving galaxies with $z > 1.5$ drawn from the sample in Paper IV were observed using NICMOS (Thompson 1992) Camera 3 in the F160W band (hereafter H_{160}). Each field was observed for a total of 3 orbits, and each orbit was split into three dithered exposures. The images reduced by the HST on-the-fly-reduction (OTFR) pipeline were retrieved from the data archive, and were corrected for various systematics such as pedestal effects, non-linearity, residual patterns, etc. These processed images were then combined into mosaics using the IRAF "DRIZZLE" task that implements the "Drizzle" algorithm of Fruchter & Hook (2002). Further details of this data set will be provided in a subsequent paper (McCarthy et al. in prep).

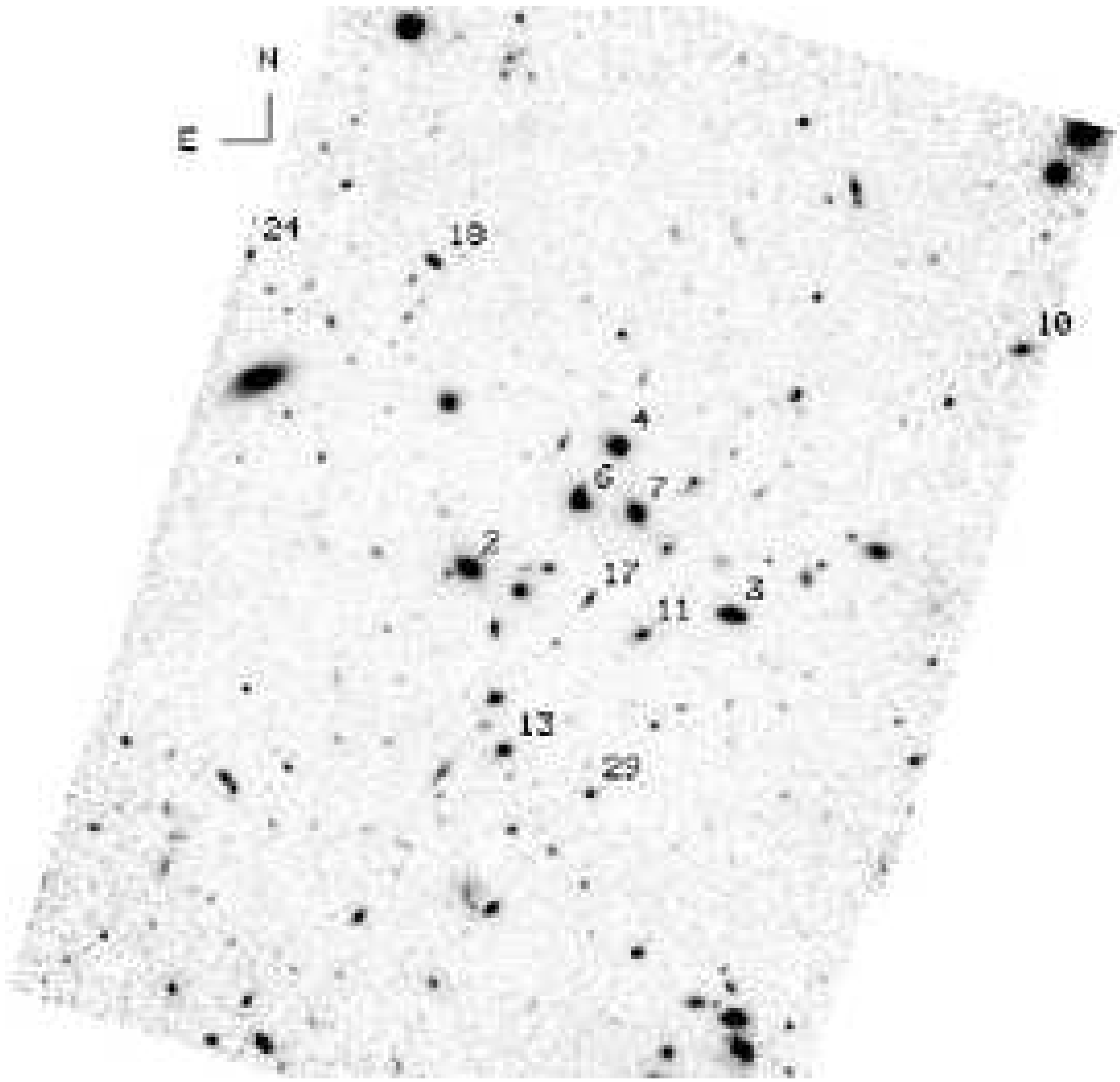

Fig. 1.— NICMOS H_{160} image of the field around GDDS-12-5869 at $z = 1.51$. The area shown is 51×72 arcseconds in extent with north at the top and east to the left. The objects listed in Table 1 are marked. GDDS-12-5869 is object # 4 while GDDS-12-5592 is object # 13. The objects are numbered in order of increasing apparent H_{160} magnitude over the entire NICMOS image, only those that we believe to be at $z = 1.5$ are marked.

2.4. Spitzer IRAC Imaging

Three of the GDDS fields were imaged with IRAC (Fazio et al. 2004) as part of a Guest Observer program. These fields were observed in all four IRAC channels, and each field was exposed for 10,842 seconds in each channel. The "Basic Calibrated Data" (BCD) products of our observations were retrieved from the *Spitzer* data archive, and were further processed to carefully remove varying backgrounds and residual patterns. These re-processed images then were combined using the MOPEX package provided by the *Spitzer* Science Center.

3. RESULTS

In Fig. 1 we show the NICMOS image of the field around GDDS-12-5869. In addition to the central luminous galaxies, the image reveals a large number of faint galaxies concentrated around them. The likely cluster members are labeled in order of increasing H_{160} magnitude. The surface density in a $20''$ radius circle to a limiting magnitude of $H_{160} = 25$ (AB) in our image is 275 arcmin^{-2}. The mean surface density of galaxies to this limit in large area random pointings is $\sim$ 60 arcmin^{-2} (e.g. Yan et al. 1999). Thus the NICMOS imaging alone reveals a $\sim 5\times$ overdensity in this field.

3.1. The Red Galaxies around GDDS-12-5869

In Figure 2 we present a color image of this field, which dramatically illustrates the compact grouping of very red galaxies in the vicinity of GDDS-12-5869. There are ten or more galaxies with very red optical-to-near-IR and optical-to-mid-IR colors within a circle of 128 kpc ($15''$) radius as illustrated by the white circle in Figure 2. As we will show below, these galaxies all have similar spectral energy distributions (SEDs) and thus are all likely cluster/group members. A number of other galaxies with similar colors appear throughout the field, several of which are also consistent with being at the same redshift.

The nature of this group of red galaxies is illuminated by the IRAC images at longer wavelengths. The central group of ~ 10 red galaxies are clearly detected in channel 3 (5.8μm), and most are also seen in the channel 4 (8.0μm). This clearly shows that they are at high redshift; the foreground of $z < 1$ galaxies drop out of the channel 3 and 4 images as these bands sample rest-frame wavelengths beyond the $1.6\mu m$ peak of the SED. This is illustrated in Figure 3 where we show the IRAC channel 3 image along side the R image.

In Figure 4, we show a $J - K$ vs. K color-magnitude diagram (CMD) for the area around

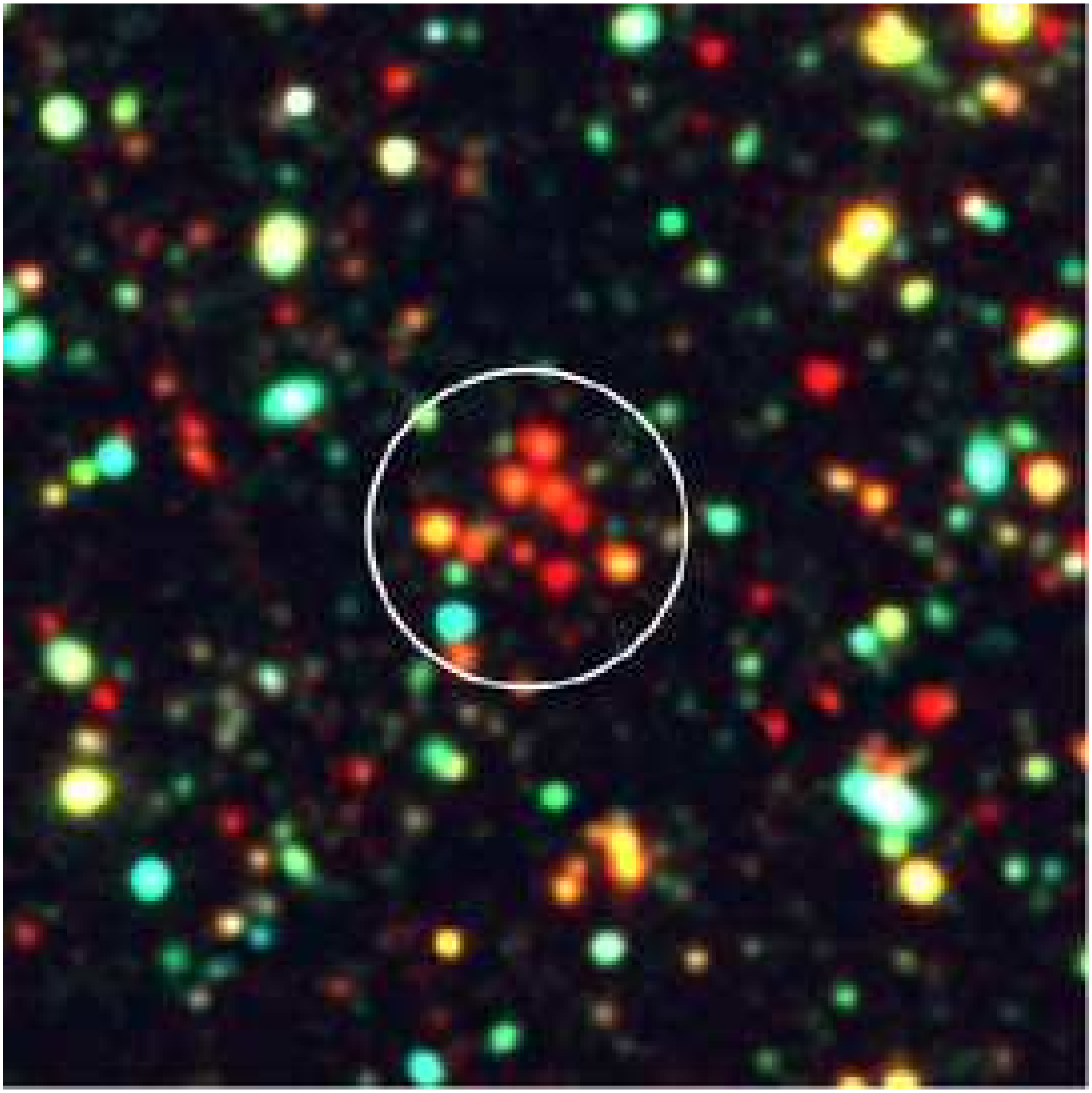

Fig. 2.— Color composite image of the GDDS-12-5869 field. The blue channel is the sum of the B & V images, the green channel is the sum of the R& I images, while the red channel combines IRAC channels 1 & 2 (3.6 and 4.5μm). The area shown is $100'' \times 100''$ in size. The diameter of the white circle is 30$''$, corresponding to 256 kpc at $z = 1.51$.

GDDS-12-5869. Only galaxies within a 300 kpc ($40''$) radius of the GDDS galaxy are shown. The dashed line is the locus of the Coma cluster color-magnitude relation (de Propris et al. 1998) transformed to $z = 1.51$ using a model with a simple stellar population (SSP) formed at $z = 5$. The locus for a non-evolving model is ~ 0.2 magnitudes redder. The CMD shows that the most luminous objects, the central four to five galaxies, have colors that lie close to the expected cluster red sequence at $z = 1.51$. The bright galaxies in this CMD are at most a few tenths of a magnitude bluer than the pure passive evolution line, suggesting that significant star formation ceased one Gyr or more before the epoch of observation.

3.2. Stellar Content of the Red Galaxies

In order to further determine which galaxies are likely at the same redshift as GDDS-12-5869 and to constrain their properties, we fit a range of population synthesis models of Bruzual & Charlot (2003) to the observed SEDs of the galaxies in this field. The SEDs were constructed using 12-band photometry obtained in ground-based B, V, R, I, $z^{'}$, J, and K, NICMOS H_{160}, and IRAC channels 1 to 4. We adopted a Chabrier initial mass function (Chabrier 2003), and confined ourselves to single components with solar abundance and exponentially declining star formation histories. The stellar mass, age, star formation time scale, and reddening were left as free parameters. We first treated the redshift as a free parameter as well, and allowed it to change at a step-size of $\Delta z = 0.1$. The photometric redshifts (z_{phot}) thus derived for the central red galaxies varied somewhat. Two of them (including GDDS-12-5869) yielded best-fit $z_{phot} = 1.4$, consistent with the spectroscopic redshift of GDDS-12-5869. The best-fit z_{phot} values for the others were mixed with some as low as $z_{phot} \sim 0.8$. Nevertheless, a redshift of 1.5 was still among the acceptable solutions for most of these objects. We then fit each of the bright red galaxies again, but forced the models to be at $z = 1.5$. For 12 galaxies we obtained best-fits with reduced chi-square ($\chi^{'2}$) values near unity. These galaxies are thus considered as candidate cluster members. Table 1 lists their best-fit model parameters obtained at a fixed redshift of $z = 1.5$, together with their measured properties. Several of the galaxies outside the central $20''$ radius circle had fits that were significantly worse at $z = 1.5$ than at sufficiently different redshifts ($|\Delta z| \geq 0.5$), and thus are unlikely to be cluster members. The total stellar mass in the 7 well measured galaxies in the central $30''$ is $\sim 6 \times 10^{11} \mathrm{M}_{\odot}$ and all of these appear to be primarily passively evolving objects at the same redshift as the GDDS galaxy.

3.3. Morphologies

Our deep HST imaging allows us to examine the structure of the red galaxies in this compact group. In Figure 6 we present expanded images of eight galaxies from Table 1 in both the H_{160}

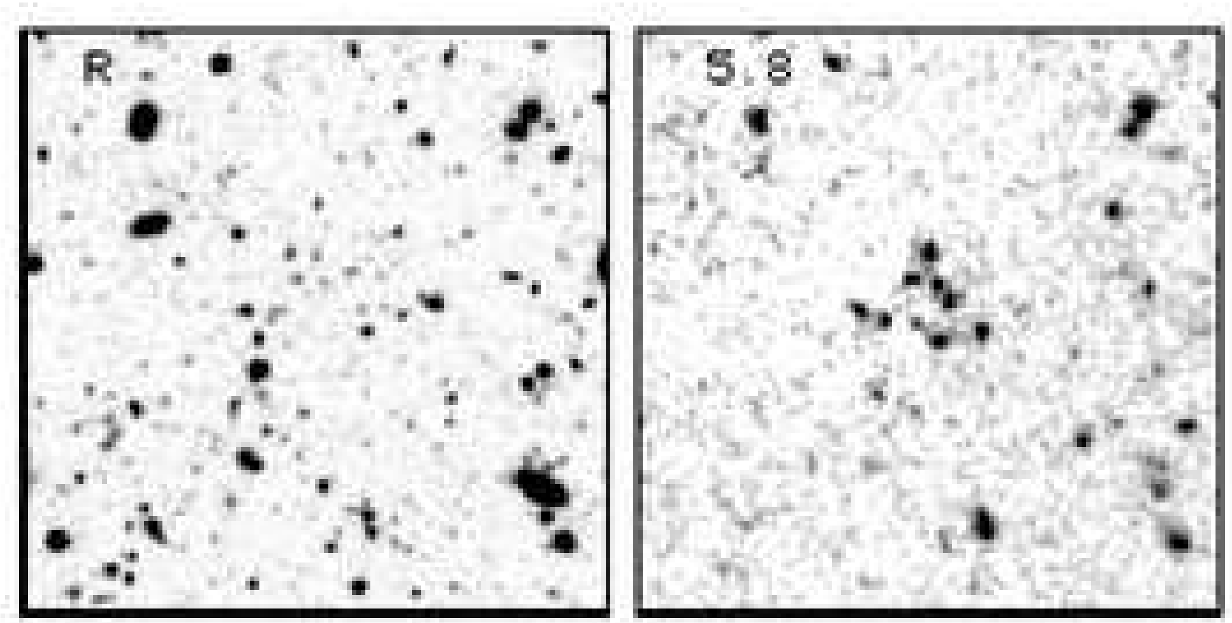

Fig. 3.— R-band (left) and IRAC channel 3 (right) images of a $2' \times 2'$ area around GDDS-12-5869. The concentration of red galaxies is most evident in IRAC channel 3 (5.8μm) as the foreground of galaxies at $z < 1$ drop out.

Table 1. Properties and Best Fit Model Parameters of Candidate Cluster Members

Object	RA	DEC	I(Vega)	K(Vega)	m(5.8μ)	Age(Gyr)	$M_\star(10^{10}M_\odot)$	χ'^2
02	12 05 22.31	-07 24 18.7	22.2	20.2	20.7	0.8	11.0	8.1
03	12 05 21.96	-07 24 22.3	22.7	20.3	20.6	0.9	9.7	2.6
04	12 05 21.54	-07 24 09.5	23.8	20.5	20.5	3.5	18.8	1.1
06	12 05 21.73	-07 24 13.6	23.3	20.7	20.9	1.4	8.2	1.0
07	12 05 21.45	-07 24 14.6	24.0	21.0	20.8	1.9	11.4	1.0
10	12 05 19.47	-07 24 02.1	25.2	21.8	21.1	0.5	8.0	1.1
11	12 05 21.42	-07 24 23.8	-	21.8	20.8	1.1	5.1	1.1
13	12 05 22.13	-07 24 32.6	23.8	21.3	21.6	1.6	4.8	1.1
17	12 05 21.69	-07 24 21.1	24.8	-	22.0	< 0.1	1.8	2.3
18	12 05 22.48	-07 23 55.4	23.9	21.8	23.1	0.6	1.7	2.3
24	12 05 23.43	-07 23 54.9	-	-	21.4	0.7	1.8	14
29	12 05 21.68	-07 24 21.7	24.5	22:	22.8	1.8	1.4	0.6

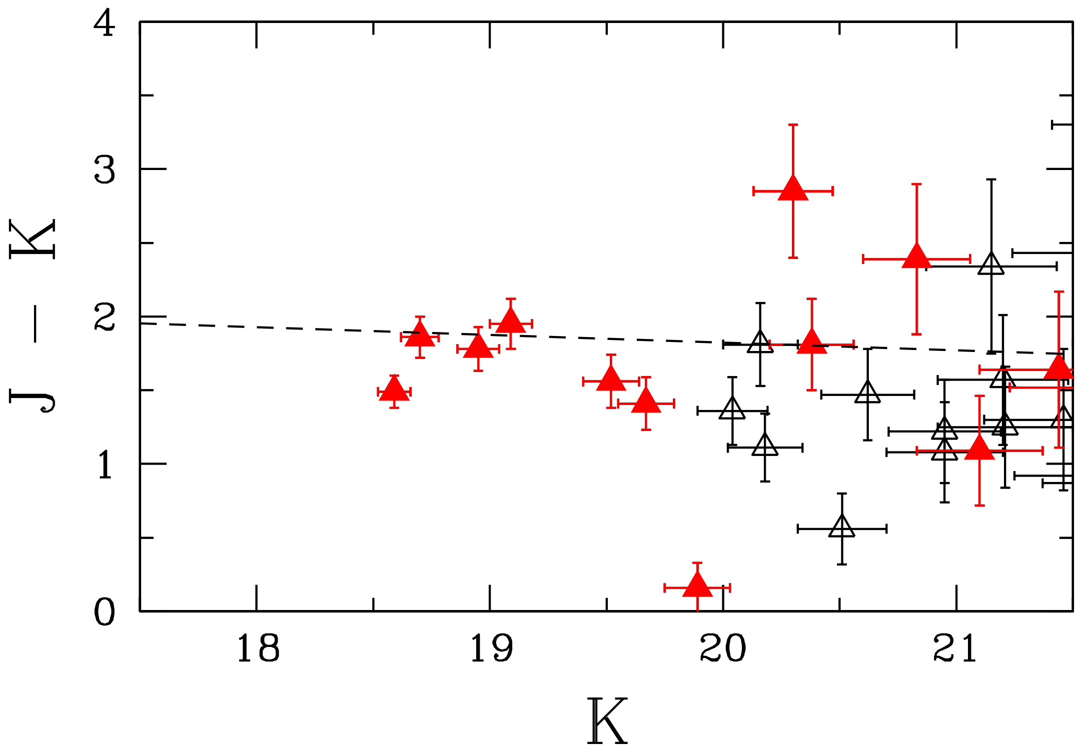

Fig. 4.— $J-K$ vs. K(Vega) color-magnitude diagram for a circular region centered on object # 17. The red points are objects within a $15''$ radius (as in Figure 1), the black symbols cover an area $30''$ in radius. The dashed line is the color-magnitude relation for the Coma cluster evolved to $z=1.51$, assuming a purely passively evolving SSP formed at a redshift of 5.

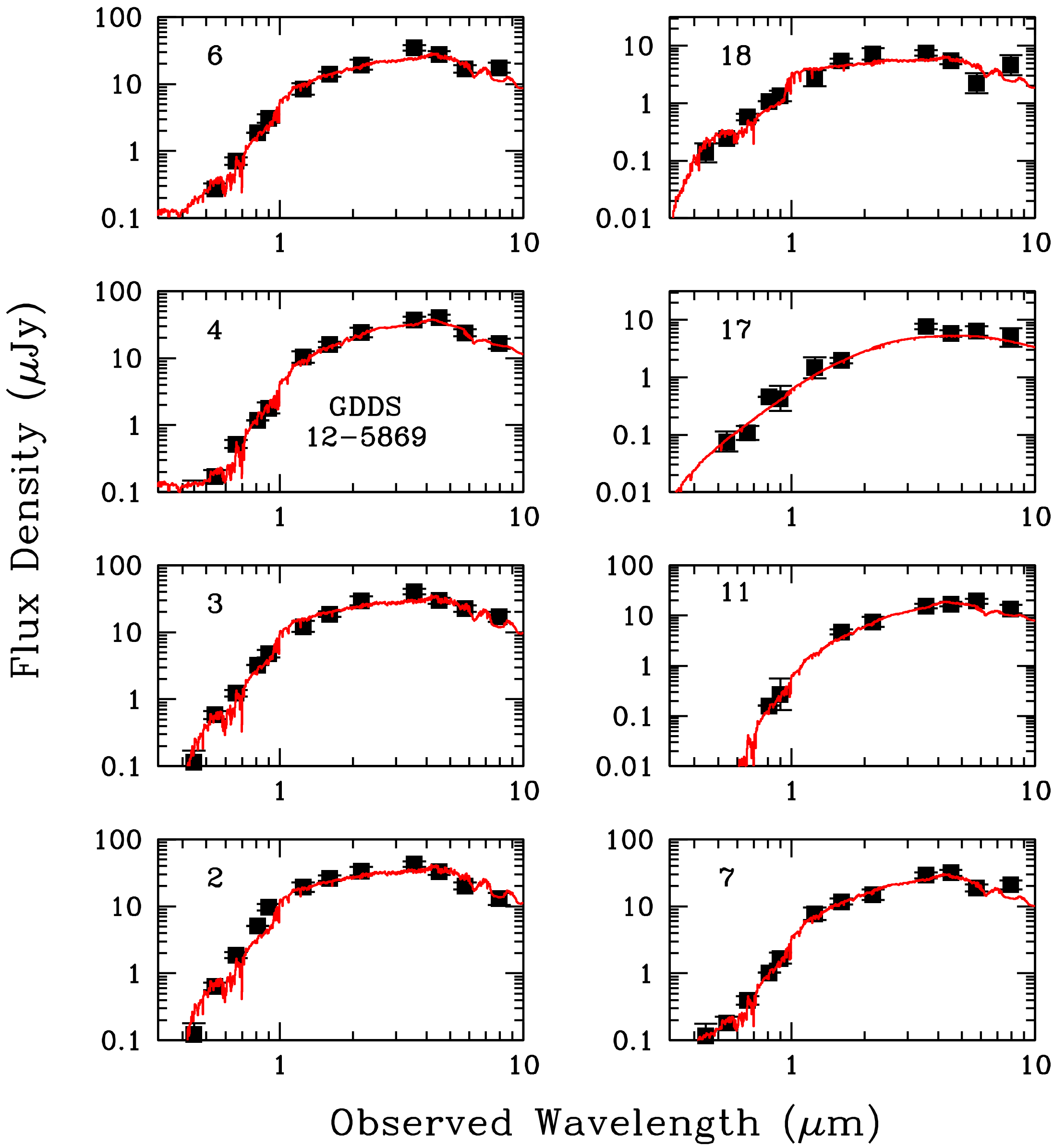

Fig. 5.— SEDs (filled squares with error bars) and best-fit models at $z = 1.5$ (solid curves) for the eight brightest candidate cluster members. GDDS-12-5869 is marked.

and I_{813} images from NICMOS and ACS respectively. Of these eight galaxies, four (Nos. 2, 4, 7, & 11) appear to be early-types, while the other four clearly show disks, although galaxies Nos. 3 and 18 appear to have large bulges. Several of the objects have close companions and galaxy No. 6 appears to be an ongoing merger of two systems. This mix of morphologies is not far from that seen in groups at intermediate redshifts, but is disk-rich compared to the cores of rich clusters today (Dressler 1980; Whitmore et al. 1993; Zabludoff & Mulchaey 1998). Two of the objects in our near-IR images are either not detected, or are marginally detected, in our deep ACS I_{814} images. These objects (Nos. 11 & 24) appear to be examples of IRAC-selected extremely red objects (IEROs; Yan et al. (2004)). The object for which we have deep Gemini spectroscopy, No. 4 in Figure 1, has the simplest morphology of all of the galaxies in the group and appears to be closest to a relaxed early type galaxy.

4. Discussion

The cluster around GDDS-12-5869 provides one of the most distant examples of a compact red sequence of massive galaxies. This system has a crossing time of ~ 0.5Gyr if the velocity dispersion is appropriate for an intermediate mass cluster (e.g. ~ 500km s^{-1}). The stellar mass enclosed within a sphere 170 kpc in radius, based on our fits, is $\sim 7 - 9 \times 10^{11}M_{\odot}$, comparable to the stellar masses of cD galaxies and to the central density of rich clusters (e.g. Henry 1989; Lewis et al. 2003). It is plausible that several of the central galaxies (e.g. nos. 4, 6, & 7) will merge in a few dynamical times and by $z \sim 0.5$ will be a typical brightest cluster galaxy. A typical M$_{total}$/M$_{stars}$ for poor clusters (e.g. ~ 50; Balogh et al. 2007) implies a total mass in the central system of $\sim 5 \times 10^{13}$M$_{\odot}$.

Dense x-ray selected groups in the local universe have comparable stellar and total masses (Mulchaey 2000) and these groups are believed to be in a short-lived state of rapid evolution. The compact grouping of red galaxies around GDDS-12-5869 may be the core of a larger structure. Our deep H_{160} image shows that there are many more faint galaxies in this system than detected in the shallower *Spitzer* images. The overdensity in our H_{160} image and the distribution of colors suggest that the red sequence may be confined to the central high density region of this system.

The total stellar mass density in the $1 < z < 2$ epoch is evolving rapidly (Dickinson et al. 2003; Glazebrook et al. 2004; Rudnick et al. 2003) and there is evidence that the mass density in early types in particular is undergoing dramatic change at redshifts ~ 1 and higher (Abraham et al. 2007). Deep spectroscopic studies also show that pure passive galaxies are becoming increasingly rare at $z \gtrsim 1.5$. Dense groups and clusters, such as the one presented here, may be the sites of the rapid growth and transformation of high mass galaxies that led to the formation of the red sequence seen at $z \sim 1$ and below (e.g. Kauffman et al 2003; Faber et al. 2006).

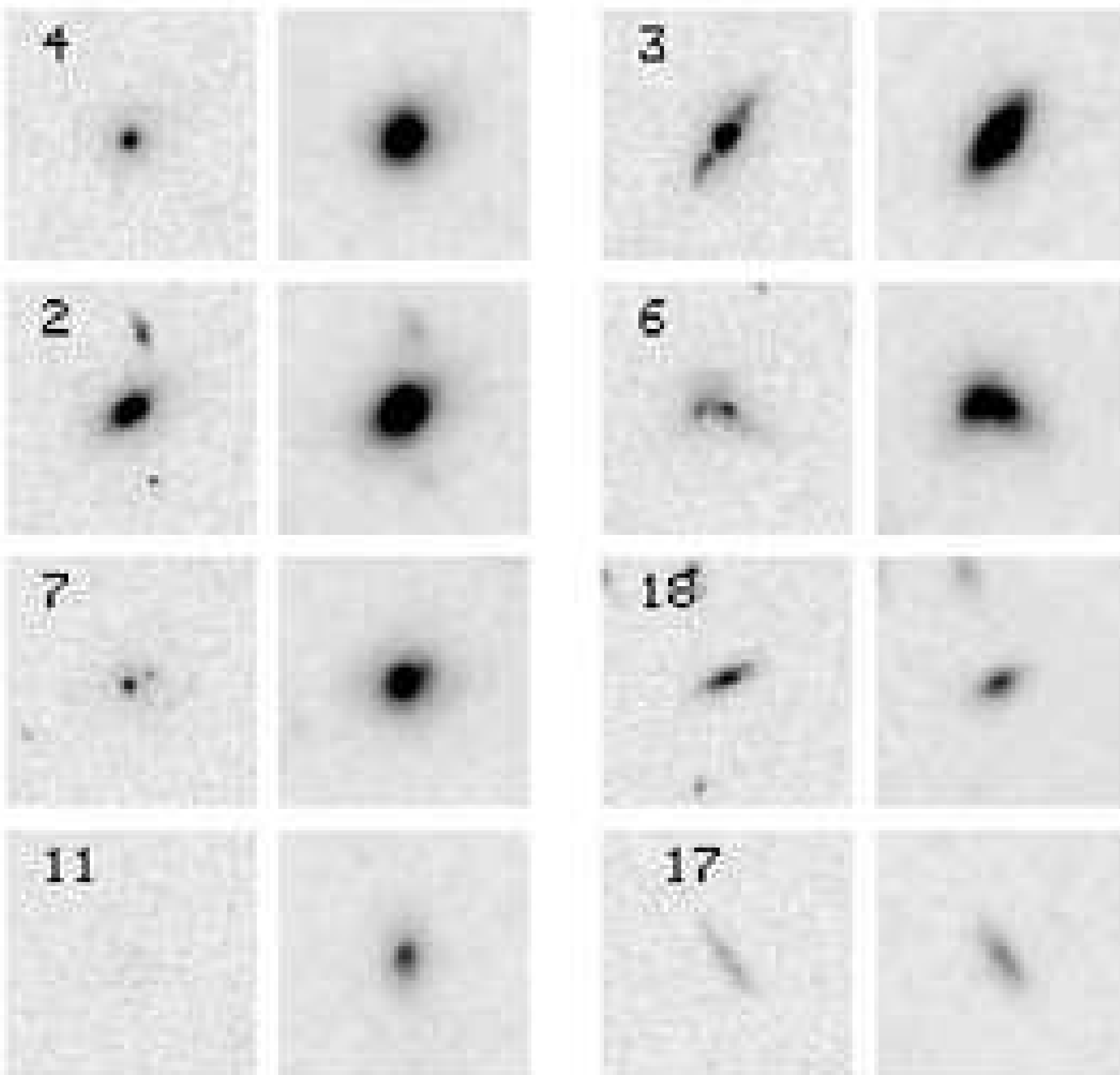

Fig. 6.— NICMOS H_{160} (right) and ACS I_{814} (left) images of cluster candidate galaxies. The objects are labeled with the same numbers from Figure 1 and Table 1. Galaxies Nos. 4 (GDDS-12-5869), 2, 11 and 7 appear to be early types, while 3, 17 and 18 are disk galaxies. Object No. 6 appears to be an active merger between two disk galaxies.

REFERENCES

Abraham, R. G., et al. 2007. In press.

Abraham, R. G., et al. 2004, AJ, 127, 2455

Balogh, M. L., Wilman, D., Hendeson, R. D. E., Bower, R. G., Gilbank, D., Whitaker, R., Morris, S., Hau, G. 2007, MNRAS, in press (astro-ph/0610839)

Bruzual, G., & Charlot, S. 2003, MNRAS, 344, 1000

Chabrier, G. 2003, PASP, 115, 763

Chen, H.-W., et al. 2002, ApJ, 570, 54

de Propris, R., Eisenhardt, P. R., Stanford, S. A., & Dickinson, M. 1998, ApJ, 503, L45

Dickinson, M., Papovich, C., Ferguson, H. C., & Budavári, T. 2003, ApJ, 587, 25

Dressler, A. 1980, ApJ, 236, 351

Faber, S. M., et al. 2007 ApJ, in press (astro-ph/0506044)

Fazio, G. G., et al. 2004, ApJS, 154, 10

Firth, A. E., et al. 2002, MNRAS, 332, 617

Fruchter, A. S., & Hook, R. N. 2002, PASP, 114, 144

Gladders, M. D., & Yee, H. K. C. 2005, ApJS, 157, 1

Glazebrook, K., et al. 2004, Nature, 430, 181

Kauffman, G., et al. 2003, MNRAS, 341, 54

Kelson, D. D., Illingworth, G. D., van Dokkum, P. G., & Franx, M. 2000, ApJ, 531, 137

Koekemoer, A. M.; Fruchter, A. S.; Hook, R. N.; Hack, W. 2002, Proceedings of the 2002 HST Calibration Workshop (eds. Santiago Arribas, Anton Koekemoer & Brad Whitemore), p.337

McCarthy, P. J., et al. 2001, ApJ, 560, L131

McCarthy, P. J., et al. 2004, ApJ, 614, L9

Mulchaey, J. S. 2000, ARA&A, 38, 289

Rostatti, P., Borgani, S., Della Cella, R., Burg, R. Norman, C., Giacconi, R. 1998, ApJ492, 21

Rudnick, G., et al. 2003, ApJ, 599, 847

Springel, V., et al. 2005, Nature, 435, 629

Stanford, S. A., Eisenhardt, P. R., & Dickinson, M. 1998, ApJ, 492, 461

Stanford, S. A., et al. 2005, ApJ, 634, L129

Stanford, S. A., et al. 2006, ApJ, 646, L13

Thompson, R. 1992, Space Science Reviews, 61, 69

van Dokkum, P. G., Franx, M., Kelson, D. D., & Illingworth, G. D. 1998, ApJ, 504, L17

Whitford, B. C., Gilmore, D. M., & Jones, C. 1993, ApJ, 407, 489

Yan, L., et al. 1999, ApJ, 519, L47

Yan, H., et al. 2004, ApJ, 616, 63

Zabludoff, A. I., & Mulchaey, J. S. 1998, ApJ, 496, 39